

THE P_1^{mod} ELEMENT: A NEW NONCONFORMING FINITE ELEMENT FOR CONVECTION-DIFFUSION PROBLEMS*

PETR KNOBLOCH[†] AND LUTZ TOBISKA[‡]

Abstract. We consider a nonconforming streamline diffusion finite element method for solving convection-diffusion problems. The loss of the Galerkin orthogonality of the streamline diffusion method when applied to nonconforming finite element approximations results in an additional error term which cannot be estimated uniformly with respect to the perturbation parameter for the standard piecewise linear or rotated bilinear elements. Therefore, starting from the Crouzeix–Raviart element, we construct a modified nonconforming first order finite element space on shape regular triangular meshes satisfying a patch test of higher order. A rigorous error analysis of this P_1^{mod} element applied to a streamline diffusion discretization is given. The numerical tests show the robustness and the high accuracy of the new method.

Key words. convection-diffusion problems, streamline diffusion method, nonconforming finite elements, error estimates

AMS subject classifications. 65N30, 65N15

PII. S0036142902402158

1. Introduction. We consider the convection-diffusion equation

$$(1.1) \quad -\varepsilon \Delta u + \mathbf{b} \cdot \nabla u + cu = f \quad \text{in } \Omega, \quad u = u_b \quad \text{on } \partial\Omega,$$

where $\Omega \subset \mathbb{R}^2$ is a bounded domain with a polygonal boundary $\partial\Omega$, $\varepsilon \in (0, 1)$ is constant, $\mathbf{b} \in W^{1,\infty}(\Omega)^2$, $c \in L^\infty(\Omega)$, $f \in L^2(\Omega)$, and $u_b \in H^{3/2}(\partial\Omega)$. We assume that

$$(1.2) \quad c - \frac{1}{2} \operatorname{div} \mathbf{b} \geq c_0,$$

where c_0 is a positive constant. This assumption guarantees that (1.1) admits a unique solution for all positive values of the parameter ε .

In the convection dominated case, in which $\varepsilon \ll 1$, the standard Galerkin finite element method produces unphysical oscillations if the local mesh size is not small enough. Among several possible remedies for this undesirable behavior, the streamline diffusion method [8], [15] attracted considerable attention over the last decade, in particular because of its structural simplicity, generality, and the quality of the numerical solution. Summarizing the existing literature we come to the conclusion that in the case of conforming finite element approximations the convergence properties of the streamline diffusion methods are well understood; see, e.g., [6], [10], [14], [15], [18]. Particularly, using piecewise polynomial approximations of degree k in the convection dominated regime ($\varepsilon \leq h$), one can prove the error estimate

$$(1.3) \quad \| \|u - u_h\| \| \leq Ch^{k+1/2} \|u\|_{k+1,\Omega},$$

*Received by the editors February 5, 2002; accepted for publication (in revised form) September 27, 2002; published electronically April 23, 2003.

<http://www.siam.org/journals/sinum/41-2/40215.html>

[†]Faculty of Mathematics and Physics, Institute of Numerical Mathematics, Charles University, Sokolovská 83, 186 75 Praha 8, Czech Republic (knobloch@karlin.mff.cuni.cz). The research of this author was supported by the European Science Foundation (Programme AMIF—Applied Mathematics for Industrial Flow Problems), by the Czech Grant Agency under grants 201/99/P029 and 201/99/0267, and by grant MSM 113200007.

[‡]Institut für Analysis und Numerik, Otto–von–Guericke–Universität Magdeburg, Postfach 4120, 39016 Magdeburg, Germany (tobiska@mathematik.uni-magdeburg.de).

where $||| \cdot |||$ denotes the streamline diffusion norm defined in section 3.

The situation changes dramatically if nonconforming finite element approximations are used. Finite element methods of nonconforming type are attractive in computational fluid dynamics since they easily fulfill the Babuška–Brezzi condition. Moreover, because of their edge-oriented degrees of freedom they result in cheap local communication when implementing the method on a MIMD-machine (cf. [5], [9], [16]). Unfortunately, compared to conforming approximations much less is known about the convergence properties of streamline diffusion-type methods for nonconforming finite element approximations.

It has been shown in [12] that special care is necessary to prove the error estimate (1.3) in the nonconforming case. Indeed, when considering nonconforming approximation spaces we lose the continuity property over inner element edges, and the coercivity of the corresponding bilinear form depends on the type of discretization for the convective term. Our assumptions guarantee that the bilinear form with the so-called skew-symmetric discretization of the convective term (cf. the bilinear form a_h^{skew} in section 3) is always coercive in contrast to the convective form (cf. the bilinear form a_h^{conv} in subsection 4.1). On the other hand, the skew-symmetric form leads to an additional term in the consistency error which is difficult to estimate uniformly in ε . In [11], [12] these difficulties have been overcome by adding some special jump terms and thus modifying the standard streamline diffusion finite element method. However, a drawback of these jump terms is that they decrease the sparsity of the stiffness matrix and that they are difficult to implement. So we would like to avoid the jump terms, but then the coercivity of the convective bilinear form is open in general. Recently, it has been discovered in [17] that this coercivity can be guaranteed for the nonconforming rotated bilinear element on rectangular meshes if $|\mathbf{b}|_{1,\infty,\Omega}$ is small compared to c_0 . Unfortunately, a similar result is not true for the nonconforming linear triangular Crouzeix–Raviart element [4], not even on three-directional meshes. However, also in cases when the convective bilinear form is coercive, the optimal order $O(h^{k+1/2})$ cannot be shown in general. For example, in [17] a superconvergence property on uniform meshes was necessary to prove an ε -uniform convergence result of optimal order $O(h^{3/2})$. Thus, summarizing the known results we see that in general, without using jump terms and on general meshes, we cannot guarantee the same optimal convergence results as in the conforming case.

Particularly, our numerical experiences show that, in the convection dominated regime, it is often not possible to obtain an acceptable accuracy using the mentioned Crouzeix–Raviart element combined with the standard streamline diffusion discretization. In fact, this method is—even for smooth functions—not ε -uniformly convergent. Therefore, the aim of this paper is to develop a first order nonconforming method on general triangular meshes which guarantees the same optimal convergence properties as in the conforming case but does not employ any modifications (such as the above jump terms) of the standard streamline diffusion method. Let us mention that our ideas are not restricted to the first order of accuracy and that an extension to higher order methods is straightforward.

Our method is based on using the standard streamline diffusion discretization with the skew-symmetric form of the convective term and on introducing a new nonconforming finite element space. The theoretical analysis presented in this paper shows that the optimal convergence order known from the conforming finite element method can be recovered if the nonconforming space satisfies a patch test of order 3 since then a better estimate of the consistency error can be obtained. We shall construct such a space by enriching the Crouzeix–Raviart space by suitable nonconforming bubble

functions and by restricting the enlarged space to its subspace of functions satisfying the patch test of order 3. The finite element space obtained in such a way contains *modified* Crouzeix–Raviart functions and therefore we call this new element the P_1^{mod} element. This new element not only guarantees the optimal convergence order but also leads to very robust discretizations and much more accurate results than the Crouzeix–Raviart element. In addition, the iterative solver used to compute the discrete solution converges much faster than for the Crouzeix–Raviart element. Let us also mention that the P_1^{mod} element satisfies a discrete Korn inequality (cf. [13]), which is not true for most first order nonconforming finite elements, including the Crouzeix–Raviart element.

The enrichment of the Crouzeix–Raviart space by bubble functions may resemble the techniques where the bubble functions are used to recover various stabilized methods and to find a reasonable rule for the choice of the stabilizing parameters (cf., e.g., [1], [2]). However, our approach is completely different since we start from a stabilized method and the bubble functions are added not to replace the stabilization but to provide an additional stability. In addition, the bubble functions are coupled with the Crouzeix–Raviart functions so that they cannot be eliminated from the discrete problem.

The paper is organized in the following way. Section 2 introduces various notation which will be used in the subsequent sections. In section 3, we recall the weak formulation of (1.1) and describe a nonconforming streamline diffusion finite element discretization. Then the error analysis is presented in section 4. Section 5 is devoted to the construction of the P_1^{mod} element. Section 6 shows that the piecewise linear part of a P_1^{mod} discrete solution asymptotically behaves in the same way as the discrete solution itself, which is useful for postprocessing. Finally, in section 7, we present numerical results which demonstrate the good behavior of discretizations employing the P_1^{mod} element.

2. Notation. We assume that we are given a family $\{\mathcal{T}_h\}$ of triangulations of the domain Ω parametrized by a positive parameter $h \rightarrow 0$. Each triangulation \mathcal{T}_h consists of a finite number of closed triangular elements K such that $h_K \equiv \text{diam}(K) \leq h$, $\bar{\Omega} = \bigcup_{K \in \mathcal{T}_h} K$, and any two different elements $K, \tilde{K} \in \mathcal{T}_h$ are either disjoint or possess either a common vertex or a common edge. In order to prevent the elements from degenerating when h tends to zero, we assume that the family of triangulations is regular; i.e., there exists a constant C independent of h such that

$$\frac{h_K}{\varrho_K} \leq C \quad \forall K \in \mathcal{T}_h, \quad h > 0,$$

where ϱ_K is the maximum diameter of circles inscribed into K .

We denote by \mathcal{E}_h the set of edges E of \mathcal{T}_h . The set of inner edges will be denoted by \mathcal{E}_h^i and the set of boundary edges by \mathcal{E}_h^b . Further, we denote by h_E the length of the edge E and by S_E the union of the elements adjacent to E (i.e., S_E consists of one or two elements). For any edge E , we choose a fixed unit normal vector \mathbf{n}_E to E . If $E \in \mathcal{E}_h^b$, then \mathbf{n}_E coincides with the outer normal vector to $\partial\Omega$. Consider any $E \in \mathcal{E}_h^i$, and let K, \tilde{K} be the two elements possessing the edge E denoted in such a way that \mathbf{n}_E points into \tilde{K} . If v is a function belonging to the space

$$H^{1,h}(\Omega) = \{v \in L^2(\Omega); v|_K \in H^1(K) \quad \forall K \in \mathcal{T}_h\},$$

then we define the jump of v across E by

$$(2.1) \quad [[v]]_E = (v|_K)|_E - (v|_{\tilde{K}})|_E.$$

If $E \in \mathcal{E}_h^b$, then we set $[[v]]_E = v|_E$, which is the jump defined by (2.1) with v extended by zero outside Ω .

To formulate a streamline diffusion method for (1.1), we need finite element functions which are piecewise H^2 . We assume this regularity with respect to subdivisions of the elements of the triangulation only, which allows more flexibility in the construction of finite element spaces approximating $H_0^1(\Omega)$ (cf. Remark 5.1). The subdivisions can be defined using a triangulation $\widehat{\mathcal{G}}$ of the standard reference element \widehat{K} , and we assume that the set $\widehat{\mathcal{G}}$ is invariant under affine regular mappings of \widehat{K} onto \widehat{K} . Then, for any element $K \in \mathcal{T}_h$, we can introduce a subdivision

$$\mathcal{G}_K = \{F_K(\widehat{G}); \widehat{G} \in \widehat{\mathcal{G}}\},$$

where $F_K : \widehat{K} \rightarrow K$ is any affine regular mapping which maps \widehat{K} onto K . In view of the invariance of the triangulation $\widehat{\mathcal{G}}$, the set \mathcal{G}_K is independent of the choice of F_K . The space of piecewise H^2 functions with respect to the above subdivision of \mathcal{T}_h will be denoted by

$$H_{\widehat{\mathcal{G}}}^{2,h}(\Omega) = \{v \in L^2(\Omega); v|_G \in H^2(G) \quad \forall G \in \mathcal{G}_K, K \in \mathcal{T}_h\}.$$

In the following sections, we shall also need the spaces

$$\begin{aligned} \widetilde{V}_h^{conf} &= \{v_h \in C(\overline{\Omega}); v_h|_K \in P_1(K) \quad \forall K \in \mathcal{T}_h\}, & V_h^{conf} &= \widetilde{V}_h^{conf} \cap H_0^1(\Omega), \\ V_h^{nc} &= \left\{ v_h \in L^2(\Omega); v_h|_K \in P_1(K) \quad \forall K \in \mathcal{T}_h, \int_E [[v_h]]_E d\sigma = 0 \quad \forall E \in \mathcal{E}_h \right\}, \end{aligned}$$

and we shall denote by $i_h : H^2(\Omega) \rightarrow \widetilde{V}_h^{conf}$ the Lagrange interpolation operator.

Throughout the paper we use standard notation $L^p(\Omega)$, $W^{k,p}(\Omega)$, $H^k(\Omega) = W^{k,2}(\Omega)$, $C(\overline{\Omega})$, etc. for the usual function spaces; see, e.g., [3]. The norm and seminorm in the Sobolev space $W^{k,p}(\Omega)$ will be denoted by $\|\cdot\|_{k,p,\Omega}$ and $|\cdot|_{k,p,\Omega}$, respectively, and we set $\|\cdot\|_{k,\Omega} = \|\cdot\|_{k,2,\Omega}$ and $|\cdot|_{k,\Omega} = |\cdot|_{k,2,\Omega}$. For the space $H^{1,h}(\Omega)$, we define an analogue of $|\cdot|_{1,\Omega}$ by

$$|v|_{1,h} = \left(\sum_{K \in \mathcal{T}_h} |v|_{1,K}^2 \right)^{1/2}, \quad v \in H^{1,h}(\Omega).$$

The inner product in the space $L^2(G)$ will be denoted by $(\cdot, \cdot)_G$, and we set $(\cdot, \cdot) = (\cdot, \cdot)_\Omega$. Finally, we denote by C a generic constant independent of h and ε .

3. Weak formulation and discrete problem. Denoting by $\widetilde{u}_b \in H^2(\Omega)$ an extension of u_b , a natural weak formulation of the convection-diffusion equation (1.1) reads as follows:

Find $u \in H^1(\Omega)$ such that $u - \widetilde{u}_b \in H_0^1(\Omega)$ and

$$a(u, v) = (f, v) \quad \forall v \in H_0^1(\Omega),$$

where

$$a(u, v) = \varepsilon(\nabla u, \nabla v) + (\mathbf{b} \cdot \nabla u, v) + (cu, v).$$

This weak formulation has a unique solution.

We intend to approximate the space $H_0^1(\Omega)$ by a nonconforming finite element space V_h and at this stage we assume only that

$$(3.1) \quad V_h^{conf} \subset V_h \subset H^{1,h}(\Omega) \cap H_{\widehat{\mathcal{G}}}^{2,h}(\Omega).$$

The inclusion $V_h^{conf} \subset V_h$ ensures first order approximation properties of V_h with respect to $|\cdot|_{1,h}$ when $h \rightarrow 0$.

A finite element discretization of (1.1) could be simply obtained by using the bilinear forms

$$a_h^d(u, v) = \varepsilon \sum_{K \in \mathcal{T}_h} (\nabla u, \nabla v)_K, \quad a_h^c(u, v) = \sum_{K \in \mathcal{T}_h} (\mathbf{b} \cdot \nabla u, v)_K, \quad u, v \in H^{1,h}(\Omega),$$

instead of the first two terms in $a(u, v)$ and by replacing the space $H_0^1(\Omega)$ in the weak formulation by the finite element space V_h . However, the bilinear form corresponding to the discrete problem generally would not be coercive and therefore, before passing from the weak formulation to the discrete problem, we first apply integration by parts to the convective term $(\mathbf{b} \cdot \nabla u, v)$ to obtain

$$(\mathbf{b} \cdot \nabla u, v) = \frac{1}{2} [(\mathbf{b} \cdot \nabla u, v) - (\mathbf{b} \cdot \nabla v, u) - (\operatorname{div} \mathbf{b}, uv)], \quad u \in H^1(\Omega), v \in H_0^1(\Omega).$$

Thus, a discrete analogue of the second term in the bilinear form a also is

$$a_h^s(u, v) = \frac{1}{2} \sum_{K \in \mathcal{T}_h} [(\mathbf{b} \cdot \nabla u, v)_K - (\mathbf{b} \cdot \nabla v, u)_K - (\operatorname{div} \mathbf{b}, uv)_K], \quad u, v \in H^{1,h}(\Omega).$$

This bilinear form is skew-symmetric if $\operatorname{div} \mathbf{b} = 0$. That gives rise to the notation a_h^{skew} below. For $u \in H_{\widehat{\mathcal{G}}}^{2,h}(\Omega)$ and $v \in H^{1,h}(\Omega)$, we define a streamline diffusion term by

$$a_h^{sd}(u, v) = \sum_{K \in \mathcal{T}_h} \sum_{G \in \mathcal{G}_K} (-\varepsilon \Delta u + \mathbf{b} \cdot \nabla u + cu, \delta_K \mathbf{b} \cdot \nabla v)_G,$$

where $\delta_K \geq 0$ is a control parameter. Now, denoting

$$\begin{aligned} a_h^{skew}(u, v) &= a_h^d(u, v) + a_h^s(u, v) + (cu, v) + a_h^{sd}(u, v), \\ l_h(v) &= (f, v) + \sum_{K \in \mathcal{T}_h} (f, \delta_K \mathbf{b} \cdot \nabla v)_K, \end{aligned}$$

the streamline diffusion finite element method investigated in this paper reads as follows:

Find $u_h \in H^{1,h}(\Omega)$ such that $u_h - i_h \widetilde{u}_b \in V_h$ and

$$(3.2) \quad a_h^{skew}(u_h, v_h) = l_h(v_h) \quad \forall v_h \in V_h.$$

A natural norm for investigating the properties of the problem (3.2) is the streamline diffusion norm

$$\| \| v \| \| = \left(\sum_{K \in \mathcal{T}_h} \{ \varepsilon \|v\|_{1,K}^2 + c_0 \|v\|_{0,K}^2 + \delta_K \|\mathbf{b} \cdot \nabla v\|_{0,K}^2 \} \right)^{1/2}.$$

Using standard arguments (cf. [3, Chapter III]), we deduce that there exist constants μ_1, μ_2 independent of h such that

$$(3.3) \quad \|\Delta v_h\|_{0,G} \leq \mu_1 h_K^{-1} |v_h|_{1,G} \quad \forall v_h \in V_h, G \in \mathcal{G}_K, K \in \mathcal{T}_h,$$

$$(3.4) \quad |v_h|_{1,K} \leq \mu_2 h_K^{-1} \|v_h\|_{0,K} \quad \forall v_h \in V_h, K \in \mathcal{T}_h.$$

Assuming that the control parameter δ_K satisfies

$$(3.5) \quad 0 \leq \delta_K \leq \min \left\{ \frac{c_0}{2 \|c\|_{0,\infty,K}^2}, \frac{h_K^2}{2 \varepsilon \mu_1^2} \right\},$$

one can prove (cf. [12]) that the bilinear form a_h^{skew} is coercive, i.e.,

$$(3.6) \quad a_h^{skew}(v_h, v_h) \geq \frac{1}{2} \|v_h\|^2 \quad \forall v_h \in V_h.$$

This implies that the discrete problem (3.2) has a unique solution and that this solution does not depend on the choice of the extension \tilde{u}_b of u_b (cf. also Remark 5.2).

REMARK 3.1. *We admit $\delta_K = 0$ in (3.5) since the streamline diffusion stabilization is important in convection dominated regions only.*

4. Error analysis. If the weak solution of (1.1) satisfies $u \in H^2(\Omega)$, then it fulfills (1.1) almost everywhere in Ω . Multiplying (1.1) by $v_h \in V_h$ and integrating by parts, we infer that

$$(4.1) \quad a_h^{skew}(u, v_h) = l_h(v_h) + r_h^d(u, v_h) + r_h^s(u, v_h) \quad \forall v_h \in V_h,$$

where the consistency errors r_h^d and r_h^s are given by

$$r_h^d(u, v_h) = \varepsilon \sum_{K \in \mathcal{T}_h} \int_{\partial K} \frac{\partial u}{\partial \mathbf{n}_{\partial K}} v_h \, d\sigma = \varepsilon \sum_{E \in \mathcal{E}_h} \int_E \frac{\partial u}{\partial \mathbf{n}_E} [[v_h]]_E \, d\sigma,$$

$$r_h^s(u, v_h) = -\frac{1}{2} \sum_{K \in \mathcal{T}_h} \int_{\partial K} (\mathbf{b} \cdot \mathbf{n}_{\partial K}) u v_h \, d\sigma = -\frac{1}{2} \sum_{E \in \mathcal{E}_h} \int_E (\mathbf{b} \cdot \mathbf{n}_E) u [[v_h]]_E \, d\sigma$$

with $\mathbf{n}_{\partial K}$ denoting the unit outer normal vector to the boundary of K . For estimating the consistency errors, we shall use the following lemma.

LEMMA 4.1. *For any edge $E \in \mathcal{E}_h$ and any integer $k \geq 0$, let \mathcal{M}_E^k be the projection operator from $L^2(E)$ onto $P_k(E)$ defined by*

$$\int_E q \mathcal{M}_E^k v \, d\sigma = \int_E q v \, d\sigma \quad \forall q \in P_k(E), v \in L^2(E).$$

Then there exists a constant C independent of E and h such that

$$(4.2) \quad \left| \int_E \varphi (v - \mathcal{M}_E^k v) \, d\sigma \right| \leq C h_E^{k+1} |\varphi|_{1,K} |v|_{k+1,K}$$

for all $K \in \mathcal{T}_h$, $E \subset \partial K$, $\varphi \in H^1(K)$, and $v \in H^{k+1}(K)$.

Proof. See [4, Lemma 3]. \square

Now we are in a position to prove a convergence result for the discrete problem (3.2).

THEOREM 4.2. *Let the assumptions (3.1) and (3.5) be fulfilled, and let the space V_h satisfy the patch test of order $k + 1$, i.e.,*

$$(4.3) \quad \int_E [[v_h]]_E q \, d\sigma = 0 \quad \forall v_h \in V_h, q \in P_k(E), E \in \mathcal{E}_h,$$

where $k \geq 0$ is a given integer. Let the weak solution of (1.1) belong to $H^m(\Omega)$, let $m = \max\{2, k + 1\}$, and let $\mathbf{b} \in W^{k+1, \infty}(\Omega)^2$. Then the discrete solution u_h satisfies

$$(4.4) \quad |||u - u_h||| \leq C h \left(\sum_{K \in \mathcal{T}_h} \gamma_K |u|_{2,K}^2 \right)^{1/2} + C h^k \left(\sum_{E \in \mathcal{E}_h} \gamma_E \|u\|_{m, S_E}^2 \right)^{1/2},$$

where

$$\gamma_K = \varepsilon + h_K^2 + \delta_K + (\max\{\varepsilon, \delta_K\})^{-1} h_K^2, \quad \gamma_E = \min \left\{ \frac{h_E^2}{\varepsilon}, 1 \right\}.$$

Proof. Denoting $w = i_h u - u$ and $w_h = i_h u - u_h$, we have $w_h \in V_h$ and it follows from (3.2) and (4.1) that

$$(4.5) \quad a_h^{skew}(w_h, v_h) = a_h^{skew}(w, v_h) + r_h^d(u, v_h) + r_h^s(u, v_h) \quad \forall v_h \in V_h.$$

Integrating by parts, we obtain for any $v_h \in V_h$

$$a_h^s(w, v_h) = -a_h^c(v_h, w) - (\operatorname{div} \mathbf{b}, w v_h) + n_h^s(w, v_h),$$

where

$$n_h^s(w, v_h) = \frac{1}{2} \sum_{E \in \mathcal{E}_h} \int_E (\mathbf{b} \cdot \mathbf{n}_E) w [[v_h]]_E \, d\sigma.$$

Hence denoting

$$a_h(w, v_h) = a_h^d(w, v_h) - a_h^c(v_h, w) + (c - \operatorname{div} \mathbf{b}, w v_h) + a_h^{sd}(w, v_h),$$

we have

$$(4.6) \quad a_h^{skew}(w, v_h) = a_h(w, v_h) + n_h^s(w, v_h).$$

Combining (4.5), (4.6), (3.6), and the triangular inequality, we infer that

$$\begin{aligned} \frac{1}{2} |||u - u_h||| &\leq \frac{1}{2} |||w||| + \sup_{v_h \in V_h} \frac{a_h(w, v_h)}{|||v_h|||} \\ &\quad + \sup_{v_h \in V_h} \frac{n_h^s(w, v_h)}{|||v_h|||} + \sup_{v_h \in V_h} \frac{r_h^d(u, v_h)}{|||v_h|||} + \sup_{v_h \in V_h} \frac{r_h^s(u, v_h)}{|||v_h|||}. \end{aligned}$$

The first two terms on the right-hand side are well known from the conforming analysis of the problem (3.2) (cf., e.g., [15]) and can be estimated by

$$(4.7) \quad \frac{1}{2} |||w||| + \sup_{v_h \in V_h} \frac{a_h(w, v_h)}{|||v_h|||} \leq C h \left(\sum_{K \in \mathcal{T}_h} \gamma_K |u|_{2,K}^2 \right)^{1/2}.$$

The remaining three terms are purely nonconforming terms. The estimation of $r_h^d(u, v_h)$ is the easiest one: In view of (4.3), we have for any $E \in \mathcal{E}_h$

$$\int_E \frac{\partial u}{\partial \mathbf{n}_E} [[v_h]]_E \, d\sigma = \int_E \left(\frac{\partial u}{\partial \mathbf{n}_E} - \mathcal{M}_E^0 \frac{\partial u}{\partial \mathbf{n}_E} \right) [[v_h]]_E \, d\sigma,$$

and hence, applying (4.2), we deduce that

$$r_h^d(u, v_h) \leq C h \varepsilon^{1/2} |u|_{2,\Omega} |||v_h|||.$$

To estimate $r_h^s(u, v_h)$, we apply (4.3) and Lemma 4.1, and we obtain

$$\begin{aligned} \int_E (\mathbf{b} \cdot \mathbf{n}_E) u [[v_h]]_E \, d\sigma &= \int_E [(\mathbf{b} \cdot \mathbf{n}_E) u - \mathcal{M}_E^k((\mathbf{b} \cdot \mathbf{n}_E) u)] [[v_h]]_E \, d\sigma \\ &\leq C h_E^{k+1} \|u\|_{k+1, S_E} |v_h|_{1, S_E}, \end{aligned}$$

where the norms over S_E are considered to be defined elementwise. Using (3.4), we derive

$$\int_E (\mathbf{b} \cdot \mathbf{n}_E) u [[v_h]]_E \, d\sigma \leq C h_E^k \|u\|_{k+1, S_E} \gamma_E^{1/2} (\varepsilon |v_h|_{1, S_E}^2 + c_0 \|v_h\|_{0, S_E}^2)^{1/2},$$

which implies that

$$r_h^s(u, v_h) \leq C h^k \left(\sum_{E \in \mathcal{E}_h} \gamma_E \|u\|_{k+1, S_E}^2 \right)^{1/2} |||v_h|||.$$

The term $n_h^s(w, v_h)$ can be estimated analogously. The only difference is that we also use the estimate $\|w\|_{k+1, S_E} \leq C h_E |w|_{2, S_E} + \min\{1, k\} \|u\|_{k+1, S_E}$. So, we get

$$(4.8) \quad n_h^s(w, v_h) \leq C h^{\max\{1, k\}} \left(\sum_{E \in \mathcal{E}_h} \gamma_E \|u\|_{m, S_E}^2 \right)^{1/2} |||v_h|||.$$

As we see, for $k = 0$, the consistency error $r_h^s(u, v_h)$ behaves worse than the term $n_h^s(w, v_h)$ and does not allow any ε -uniform convergence. Summing up all the estimates, we obtain the theorem. \square

REMARK 4.1. *The above estimate together with the condition (3.5) suggests setting*

$$\delta_K = \begin{cases} \kappa_K h_K & \text{if } h_K > \varepsilon, \\ 0 & \text{if } h_K \leq \varepsilon, \end{cases}$$

where κ_K is bounded independently of h and satisfies

$$0 < \kappa_0 \leq \kappa_K \leq \min \left\{ \frac{c_0}{2 \|c\|_{0, \infty, K}^2 h_K}, \frac{h_K}{2 \varepsilon \mu_1^2} \right\}.$$

Then $(\max\{\varepsilon, \delta_K\})^{-1} h_K^2 \leq (\min\{1, \kappa_0\})^{-1} h_K$, and hence $\gamma_K \leq C(\varepsilon + h_K)$.

Let us consider the convection dominated case $\varepsilon \leq h$, and let δ_K be defined as in Remark 4.1, which implies that $\gamma_K \leq Ch$. Since the sum over edges in (4.4) stems from the nonconformity only, we obtain for $V_h = V_h^{conf}$ the well-known estimate

$$|||u - u_h||| \leq Ch^{3/2} |u|_{2,\Omega},$$

where the constant C is independent of u, h , and ε . Therefore, the estimate is called ε -uniform. It is known that this estimate is optimal on general meshes.

For a general nonconforming space V_h satisfying the assumptions of Theorem 4.2, the estimate (4.4) leads to the ε -uniform estimate

$$(4.9) \quad |||u - u_h||| \leq Ch^{3/2} |u|_{2,\Omega} + Ch^k \|u\|_{\max\{2,k+1\},\Omega}.$$

Thus, if we use the space $V_h = V_h^{nc}$, which satisfies (4.3) for $k = 0$ only, the ε -uniform convergence order is 0. Numerical experiments really confirm this pessimistic prediction (see section 7), which suggests that it is generally a property of the method and not a consequence of an inaccurate estimation. On the other hand, the estimate (4.9) shows that the optimal ε -uniform convergence order 3/2 can be recovered if the space V_h satisfies the patch test of order 3, i.e., $k = 2$. This is an unusual requirement for a nonconforming first order finite element space, but we shall show in section 5 that such spaces can easily be constructed.

4.1. Remarks on the convective discretization. In numerical computations, one also often considers the discrete problem (3.2) with a_h^{skew} replaced by the convective bilinear form a_h^{conv} defined by

$$(4.10) \quad a_h^{conv}(u, v) = a_h^d(u, v) + a_h^c(u, v) + (cu, v) + a_h^{sd}(u, v).$$

Note that a result similar to (3.6) does not hold for this bilinear form. Indeed,

$$a_h^{conv}(v_h, v_h) \geq \frac{1}{2} |||v_h|||^2 + \frac{1}{2} \sum_{E \in \mathcal{E}_h} \int_E (\mathbf{b} \cdot \mathbf{n}_E) [|v_h^2|]_E \, d\sigma \quad \forall v_h \in V_h,$$

where the additional term is of order $O(\|v_h\|_{0,\Omega}^2/h)$ in general (cf. [17]). Of course, the coercivity is not necessary to prove the unique solvability and to establish error estimates. It would be sufficient if an inf-sup condition were satisfied, precisely, if the constants

$$(4.11) \quad \alpha_h = \inf_{w_h \in V_h^{nc}} \sup_{v_h \in V_h^{nc}} \frac{a_h^{conv}(w_h, v_h)}{|||v_h||| \, |||w_h|||}$$

could be bounded from below by some positive constant independent of h or at least with a known dependence on h . Unfortunately, this is an open problem.

Let us consider the discrete problem (3.2) with a_h^{skew} replaced by a_h^{conv} . We again set $w = i_h u - u$ and $w_h = i_h u - u_h$. To estimate the error $u - u_h = w_h - w$ it suffices to investigate w_h since w can be estimated by (4.7). Since there is no consistency error induced by the convective term, we obtain

$$\alpha_h |||w_h||| \leq \sup_{v_h \in V_h} \frac{a_h(w, v_h)}{|||v_h|||} + 2 \sup_{v_h \in V_h} \frac{n_h^s(w, v_h)}{|||v_h|||} + \sup_{v_h \in V_h} \frac{r_h^d(u, v_h)}{|||v_h|||}.$$

Hence $\alpha_h |||w_h|||$ can be estimated by the right-hand side of (4.4). However, for $k = 0$, we can apply (4.8) and hence, for δ_K defined as in Remark 4.1, we always get at least

$$|||u - i_h u||| + \alpha_h |||i_h u - u_h||| \leq Ch |u|_{2,\Omega}.$$

Moreover, for $V_h = V_h^{nc}$ and $u \in H^3(\Omega)$, we have the estimate

$$(4.12) \quad \int_E (\mathbf{b} \cdot \mathbf{n}_E) w [[v_h]]_E d\sigma \leq C h_E^3 \|u\|_{3,S_E} |v_h|_{1,S_E}$$

so that in the convection dominated case $\varepsilon \leq h$ we even obtain

$$\| |u - i_h u| \| + \alpha_h \| |i_h u - u_h| \| \leq C h^{3/2} \|u\|_{3,\Omega}.$$

Let us mention how to prove (4.12). We denote by j_h the piecewise quadratic Lagrange interpolation operator and, for any edge $E \in \mathcal{E}_h$, we set $\mathbf{b}_E = \mathcal{M}_E^0 \mathbf{b}$. Then we have for any $E \in \mathcal{E}_h$

$$(4.13) \quad \int_E (\mathbf{b} \cdot \mathbf{n}_E) w [[v_h]]_E d\sigma = \int_E ((\mathbf{b} - \mathbf{b}_E) \cdot \mathbf{n}_E) w [[v_h]]_E d\sigma \\ + \int_E (\mathbf{b}_E \cdot \mathbf{n}_E) (j_h u - u) [[v_h]]_E d\sigma + \int_E (\mathbf{b}_E \cdot \mathbf{n}_E) (i_h u - j_h u) [[v_h]]_E d\sigma.$$

The last term on the right-hand side vanishes since $i_h u - j_h u$ is even on E and $[[v_h]]_E$ is odd on E . Using Lemma 4.1, we derive for any $z \in H^1(\Omega)$

$$\int_E z [[v_h]]_E d\sigma = \int_E (z - \mathcal{M}_E^0 z) [[v_h]]_E d\sigma \leq C h_E |z|_{1,S_E} |v_h|_{1,S_E}.$$

This implies that the first two terms on the right-hand side of (4.13) can be estimated by $C h_E^3 (|u|_{2,S_E} + |u|_{3,S_E}) |v_h|_{1,S_E}$, which proves (4.12).

The above considerations suggest that, in some cases, the bilinear form a_h^{conv} may lead to better results than a_h^{skew} , particularly in the case that $\alpha_h \geq \alpha_0 > 0$ could be verified.

5. Definition of the P_1^{mod} element. We have seen above that it is desirable to construct nonconforming first order finite element spaces satisfying the patch test of a higher order than usual. In this section, we present a possible way of constructing such spaces. The idea is to enrich the space V_h^{nc} by suitable supplementary functions and then to restrict the enlarged space to its subspace of functions satisfying the patch test of a given order. Our basic requirement is that this procedure must not destroy the edge-oriented structure of the space V_h^{nc} . This construction will lead to a new finite element space containing as a subspace modified functions from V_h^{nc} . Therefore, we denote the new space V_h^{mod} , and we call the corresponding finite element the P_1^{mod} element.

We introduce the P_1^{mod} element by describing the respective shape functions on the standard reference triangle \widehat{K} . It turns out that independently of the required order of the patch test it suffices to enrich the space $P_1(\widehat{K})$ corresponding to V_h^{nc} by three functions $\widehat{b}_1, \widehat{b}_2,$ and \widehat{b}_3 associated, respectively, with the edges $\widehat{E}_1, \widehat{E}_2,$ and \widehat{E}_3 of the element \widehat{K} . This gives the space

$$P_1^{mod}(\widehat{K}) = P_1(\widehat{K}) \oplus \text{span}\{\widehat{b}_1, \widehat{b}_2, \widehat{b}_3\}.$$

We assume for $i \in \{1, 2, 3\}$ that

$$(5.1) \quad \widehat{b}_i \in H^1(\widehat{K}), \quad \widehat{b}_i|_{\partial\widehat{K} \setminus \widehat{E}_i} = 0,$$

$$(5.2) \quad \widehat{b}_i|_{\widehat{E}_i} \text{ is odd with respect to the midpoint of } \widehat{E}_i,$$

$$(5.3) \quad \int_{\widehat{E}_i} [(1 - 2\widehat{\lambda}_{i+1}) + \widehat{b}_i] \widehat{q} d\widehat{\sigma} = 0 \quad \forall \widehat{q} \in P_1(\widehat{E}_i),$$

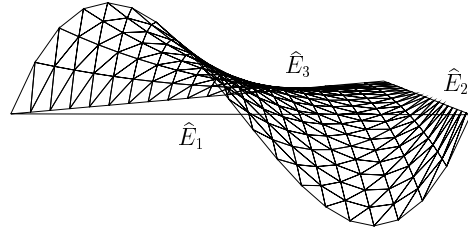


FIG. 5.1. Function $\widehat{\lambda}_2^2 \widehat{\lambda}_3 - \widehat{\lambda}_2 \widehat{\lambda}_3^2$.

where $\widehat{\lambda}_i$ is the barycentric coordinate on \widehat{K} with respect to the vertex of \widehat{K} opposite the edge \widehat{E}_i . (We set $\widehat{\lambda}_4 \equiv \widehat{\lambda}_1$.) In addition, because of the streamline diffusion method, we suppose that on the triangulation $\widehat{\mathcal{G}}$ of \widehat{K}

$$(5.4) \quad \widehat{b}_i|_{\widehat{G}} \in H^2(\widehat{G}) \quad \forall \widehat{G} \in \widehat{\mathcal{G}}.$$

Note that to verify (5.3), it suffices to prove its validity for $\widehat{q} = \widehat{\lambda}_{i+1}|_{\widehat{E}_i}$. A simple example of \widehat{b}_i satisfying the assumptions (5.1)–(5.4) is the function (cf. Figure 5.1)

$$(5.5) \quad \widehat{b}_i = 10 (\widehat{\lambda}_{i+1}^2 \widehat{\lambda}_{i+2} - \widehat{\lambda}_{i+1} \widehat{\lambda}_{i+2}^2),$$

where the indices are to be considered modulo 3.

For any element $K \in \mathcal{T}_h$, we introduce a regular affine mapping $F_K : \widehat{K} \rightarrow K$ such that $F_K(\widehat{K}) = K$ and, using this mapping, we transform the shape functions from \widehat{K} onto K . In this way, we obtain the spaces

$$P_1^{mod}(K) = P_1(K) \oplus \text{span}\{b_{K,E}|_K\}_{E \in \mathcal{E}_h, E \subset \partial K},$$

where

$$b_{K,E} = \begin{cases} \widehat{b}_i \circ F_K^{-1} & \text{in } K, \\ 0 & \text{in } \Omega \setminus K \end{cases}$$

for $E = F_K(\widehat{E}_i)$, $i = 1, 2, 3$. For each element K , we introduce six local nodal functionals

$$I_{K,E}(v) = \frac{1}{h_E} \int_E v \, d\sigma, \quad J_{K,E}(v) = \frac{3}{h_E} \int_E v (2\lambda_E - 1) \, d\sigma, \quad E \in \mathcal{E}_h, E \subset \partial K,$$

where $\lambda_E \in P_1(E)$ equals 1 at one endpoint of E and 0 at the other endpoint of E . It is easy to verify that these functionals are unisolvent with the space $P_1^{mod}(K)$. Of course, we could also use other local nodal functionals. However, we prefer the above functionals since they lead to dual basis functions having nice properties.

Now, the finite element space V_h^{mod} approximating the space $H_0^1(\Omega)$ is defined in a standard way: It consists of all functions which belong to the space $P_1^{mod}(K)$ on any element $K \in \mathcal{T}_h$, which are continuous on all inner edges in the sense of the equality of nodal functionals and for which all nodal functionals associated with boundary edges vanish. This means that

$$V_h^{mod} = \left\{ v_h \in L^2(\Omega); v_h|_K \in P_1^{mod}(K) \quad \forall K \in \mathcal{T}_h, \right. \\ \left. \int_E [[v_h]]_E q \, d\sigma = 0 \quad \forall q \in P_1(E), E \in \mathcal{E}_h \right\}.$$

For any inner edge $E \in \mathcal{E}_h^i$, we define global nodal functionals

$$I_E(v) = I_{K,E}(v), \quad J_E(v) = J_{K,E}(v),$$

where K is any element adjacent to E . (Note that, for $v \in V_h^{mod}$, the choice of K has no influence on the values of $I_{K,E}(v)$ and $J_{K,E}(v)$.) We denote by $\{\psi_E, \chi_E\}_{E \in \mathcal{E}_h^i}$ a basis of V_h^{mod} which is dual to the functionals I_E, J_E ; i.e., for any $E, E' \in \mathcal{E}_h^i$, we have

$$I_E(\psi_{E'}) = \delta_{E,E'}, \quad J_E(\psi_{E'}) = 0, \quad I_E(\chi_{E'}) = 0, \quad J_E(\chi_{E'}) = \delta_{E,E'},$$

where $\delta_{E,E'} = 1$ for $E = E'$ and $\delta_{E,E'} = 0$ for $E \neq E'$. To establish formulas for ψ_E and χ_E , we denote by K, \tilde{K} the two elements adjacent to E ; by E, E_1, E_2 the edges of K ; by E, E_3, E_4 the edges of \tilde{K} ; and by ζ_E the standard basis function of V_h^{nc} associated with the edge E (i.e., ζ_E is piecewise linear, equals 1 on E , and vanishes at the midpoints of all edges different from E). Then

$$(5.6) \quad \psi_E = \zeta_E + \beta_{E,1} b_{K,E_1} + \beta_{E,2} b_{K,E_2} + \beta_{E,3} b_{\tilde{K},E_3} + \beta_{E,4} b_{\tilde{K},E_4},$$

$$(5.7) \quad \chi_E = \beta_{E,5} b_{K,E} + \beta_{E,6} b_{\tilde{K},E},$$

where the coefficients $\beta_{E,1}, \dots, \beta_{E,6}$ are uniquely determined and equal 1 or -1 . If the functions $\hat{b}_1, \hat{b}_2, \hat{b}_3$ are chosen in a suitable way (e.g., $\hat{b}_i = \hat{b}_1 \circ \hat{F}_i$, where \hat{F}_i is an affine transformation of \hat{K} onto \tilde{K}), then $\chi_E \in H_0^1(\Omega)$, and hence the functions χ_E generate a conforming subspace of V_h^{mod} . (This is also the case for the functions χ_E presented in subsection 5.2 below.) The functions ψ_E are always purely nonconforming functions since they have jumps across the edges E_1, \dots, E_4 , and they can be viewed as modified basis functions of V_h^{nc} . In addition, from (5.6) and (5.7), it follows that, for any $v_h \in V_h^{mod}$ and any $E \in \mathcal{E}_h$, the jump $[[v_h]]_E$ is odd with respect to the midpoint of E . Therefore,

$$(5.8) \quad \int_E [[v_h]]_E q \, d\sigma = 0$$

for any even function $q \in L^1(E)$. Particularly, (5.8) holds for any $q \in P_2(E)$ vanishing at the endpoints of E . This together with the definition of V_h^{mod} implies that (5.8) holds for any $q \in P_2(E)$; i.e., the space V_h^{mod} satisfies the patch test of order 3. Moreover, if (5.3) holds for any $\hat{q} \in P_k(\hat{E}_i)$ with some $k > 1$, then it is easy to show that the basis functions ψ_E and χ_E satisfy the patch test of order $k+1$. Consequently, the whole space V_h^{mod} then satisfies the patch test of order at least $k+1$.

Let us mention that, denoting

$$(5.9) \quad B_h = \text{span}\{b_{K,E}\}_{K \in \mathcal{T}_h, E \in \mathcal{E}_h, E \subset \partial K},$$

the space V_h^{mod} can also be written as

$$V_h^{mod} = \left\{ v_h \in V_h^{nc} \oplus B_h; \int_E [[v_h]]_E q \, d\sigma = 0 \quad \forall q \in P_2(E), E \in \mathcal{E}_h \right\}.$$

Therefore, the space V_h^{mod} can be regarded as the space V_h^{nc} enriched by the nonconforming bubble functions $b_{K,E}$ and then restricted to the subspace of functions satisfying the patch test of order 3.

5.1. Properties of the modified method. As we required at the beginning, the space V_h^{mod} is an edge-oriented nonconforming finite element space possessing first order approximation properties with respect to $|\cdot|_{1,h}$. The supports of the basis functions ψ_E, χ_E are contained in the supports of the basis functions ζ_E of V_h^{nc} , and hence the space V_h^{mod} can be implemented using the same data structures as the space V_h^{nc} . In addition, owing to (5.4), the space V_h^{mod} consists of piecewise continuous functions which are continuous in the midpoints of inner edges and vanish in the midpoints of boundary edges. This is a further feature common with the space V_h^{nc} .

However, as we have shown above, there is an immense difference in the behavior of the solutions to the discrete problem (3.2) for these two spaces: Whereas no ε -uniform convergence can be shown for the space V_h^{nc} , the space V_h^{mod} guarantees the ε -uniform estimate (cf. (4.9))

$$(5.10) \quad \| \|u - u_h\| \| \leq C h^{\min\{l, 3/2\}} \|u\|_{l+1, \Omega}, \quad l = 1, 2.$$

Thus, for $u \in H^3(\Omega)$, we get the optimal ε -uniform convergence order $3/2$. Moreover, numerical tests indicate that discretizations using the space V_h^{mod} are much more accurate than those ones using the space V_h^{nc} (cf. section 7).

The price we pay for the ε -uniform estimate (5.10) is that $\dim V_h^{mod} = 2 \dim V_h^{nc}$ and that, consequently, the stiffness matrix corresponding to V_h^{mod} is generally four times larger than the one corresponding to V_h^{nc} . However, this does not mean that using the space V_h^{mod} is more expensive than using the space V_h^{nc} since typically a prescribed accuracy can be attained with the space V_h^{mod} on much coarser meshes than with the space V_h^{nc} .

The number of nonzero entries of the stiffness matrix corresponding to the space V_h^{mod} can be reduced to about 80% by using functions $\widehat{b}_1, \widehat{b}_2, \widehat{b}_3$ with disjoint interiors of their supports (cf. Remark 5.1 below). In this case, the functions χ_E can be easily eliminated from the discrete problem by static condensation. That halves the number of unknowns and reduces the number of nonzero entries to about 65%.

The dimension of the space V_h^{mod} is asymptotically the same as for the nonconforming piecewise quadratic element [7]. Since this element has second order approximation properties with respect to $|\cdot|_{1,h}$ one would expect a faster convergence than for the P_1^{mod} element. However, the element of [7] satisfies the patch test of order 2 only, and hence the corresponding consistency error tends to zero with the ε -uniform convergence order 1 (cf. the second term in (4.4)). Consequently, the ε -uniform convergence order of the discrete solution is at most 1 in the convection dominated case, whereas we have $3/2$ for the P_1^{mod} element. Note also that the P_1^{mod} element is more suitable for a parallel implementation than the element of [7].

REMARK 5.1. *Functions $\widehat{b}_1, \widehat{b}_2, \widehat{b}_3$ with disjoint interiors of their supports mentioned above can be obtained in the following way. We divide the reference triangle \widehat{K} into three subtriangles by connecting the barycenter of \widehat{K} with the vertices of \widehat{K} and denote by \widehat{K}_i the subtriangle adjacent to the edge \widehat{E}_i , $i = 1, 2, 3$. Then we require that \widehat{b}_i vanishes outside the subtriangle \widehat{K}_i . On \widehat{K}_i , the function \widehat{b}_i can be defined, e.g., by (5.5), where $\widehat{\lambda}_{i+1}$ and $\widehat{\lambda}_{i+2}$ are now considered as barycentric coordinates on \widehat{K}_i with respect to the endpoints of \widehat{E}_i . If we set $\widehat{\mathcal{G}} = \{\widehat{K}_1, \widehat{K}_2, \widehat{K}_3\}$, then all the assumptions on \widehat{b}_i made above are satisfied. Note that generally $\widehat{b}_i \notin H^2(\widehat{K})$ so that the assumption that finite element functions are piecewise H^2 only with respect to a subdivision of \mathcal{T}_h really has a practical importance.*

REMARK 5.2. *In the discrete problem (3.2), inhomogenous Dirichlet boundary conditions are represented by the condition $u_h - i_h \widetilde{u}_b \in V_h$. This is equivalent to*

$u_h - \tilde{u}_{bh} \in V_h$, where $\tilde{u}_{bh} \in H^{1,h}(\Omega)$ is any function satisfying $\tilde{u}_{bh} - i_h \tilde{u}_b \in V_h$. Now let us consider the P_1^{mod} element. If we extend the definitions of the global nodal functionals I_E, J_E and the basis functions ψ_E, χ_E to boundary edges, then

$$i_h \tilde{u}_b = \sum_{E \in \mathcal{E}_h} I_E(i_h \tilde{u}_b) \psi_E + J_E(i_h \tilde{u}_b) \chi_E.$$

Thus, the inhomogenous Dirichlet boundary conditions can be implemented by setting

$$\tilde{u}_{bh} = \sum_{E \in \mathcal{E}_h^b} I_E(i_h \tilde{u}_b) \psi_E + J_E(i_h \tilde{u}_b) \chi_E.$$

It is easy to see that then \tilde{u}_{bh} does not depend on the choice of the extension \tilde{u}_b of u_b .

5.2. Simple representation of the basis functions ψ_E and χ_E . Let us close this section by returning to the example of \tilde{b}_i given in (5.5) and rewriting the formulas (5.6), (5.7) for this particular case. We denote by K and \tilde{K} the two elements adjacent to an edge $E \in \mathcal{E}_h^i$ and by λ_1, λ_2 and $\tilde{\lambda}_1, \tilde{\lambda}_2$ the barycentric coordinates on K and \tilde{K} with respect to the endpoints of E . Further, we respectively denote by λ_3 and $\tilde{\lambda}_3$ the remaining barycentric coordinates on K and \tilde{K} . Then

$$\psi_E = \begin{cases} 1 - 2\lambda_3 - 10(\lambda_1^2 \lambda_3 - \lambda_1 \lambda_3^2) - 10(\lambda_2^2 \lambda_3 - \lambda_2 \lambda_3^2) & \text{in } K, \\ 1 - 2\tilde{\lambda}_3 - 10(\tilde{\lambda}_1^2 \tilde{\lambda}_3 - \tilde{\lambda}_1 \tilde{\lambda}_3^2) - 10(\tilde{\lambda}_2^2 \tilde{\lambda}_3 - \tilde{\lambda}_2 \tilde{\lambda}_3^2) & \text{in } \tilde{K} \setminus E, \\ 0 & \text{in } \Omega \setminus \{K \cup \tilde{K}\}, \end{cases}$$

and, after dividing by 10,

$$\chi_E = \begin{cases} \lambda_1^2 \lambda_2 - \lambda_1 \lambda_2^2 & \text{in } K, \\ \tilde{\lambda}_1^2 \tilde{\lambda}_2 - \tilde{\lambda}_1 \tilde{\lambda}_2^2 & \text{in } \tilde{K} \setminus E, \\ 0 & \text{in } \Omega \setminus \{K \cup \tilde{K}\}. \end{cases}$$

These basis functions were used in the numerical calculations presented in section 7.

6. Convergence of the piecewise linear part u_h^{lin} of u_h . Let us consider the discrete problem (3.2) with $V_h = V_h^{mod}$. Then the discrete solution u_h belongs to $\tilde{V}_h^{nc} \oplus B_h$, where

$$\tilde{V}_h^{nc} = \left\{ v_h \in L^2(\Omega); v_h|_K \in P_1(K) \quad \forall K \in \mathcal{T}_h, \quad \int_E [[v_h]]_E d\sigma = 0 \quad \forall E \in \mathcal{E}_h^i \right\}$$

and B_h was defined in (5.9). Thus, u_h can be uniquely decomposed into its piecewise linear part $u_h^{lin} \in \tilde{V}_h^{nc}$ and its bubble part $u_h^{bub} \in B_h$, i.e.,

$$u_h = u_h^{lin} + u_h^{bub}.$$

We shall show that u_h^{lin} converges to the weak solution with the same convergence order as u_h . First, let us prove the following orthogonality result.

LEMMA 6.1. *The spaces \tilde{V}_h^{nc} and B_h are orthogonal with respect to the $H_0^1(\Omega)$ inner product, i.e.,*

$$(6.1) \quad \sum_{K \in \mathcal{T}_h} (\nabla v_h, \nabla b_h)_K = 0 \quad \forall v_h \in \tilde{V}_h^{nc}, b_h \in B_h.$$

Consequently,

$$(6.2) \quad |v_h|_{1,h}^2 + |b_h|_{1,h}^2 = |v_h + b_h|_{1,h}^2 \quad \forall v_h \in \tilde{V}_h^{nc}, b_h \in B_h.$$

Moreover, for any element $K \in \mathcal{T}_h$ and any $\mathbf{a} \in \mathbb{R}^2$, we have

$$(6.3) \quad \|\mathbf{a} \cdot \nabla v_h\|_{0,K}^2 + \|\mathbf{a} \cdot \nabla b_h\|_{0,K}^2 = \|\mathbf{a} \cdot \nabla(v_h + b_h)\|_{0,K}^2 \quad \forall v_h \in \tilde{V}_h^{nc}, b_h \in B_h.$$

Proof. For any $v_h \in \tilde{V}_h^{nc}$, $b_h \in B_h$, $i, j \in \{1, 2\}$, and $K \in \mathcal{T}_h$, we derive

$$\int_K \frac{\partial v_h}{\partial x_i} \frac{\partial b_h}{\partial x_j} dx = - \int_K \frac{\partial^2 v_h}{\partial x_i \partial x_j} b_h dx + \int_{\partial K} \frac{\partial(v_h|_K)}{\partial x_i} (\mathbf{n}_{\partial K})_j b_h|_K d\sigma = 0.$$

Hence we obtain (6.1) and also

$$(\mathbf{a} \cdot \nabla v_h, \mathbf{a} \cdot \nabla b_h)_K = 0 \quad \forall v_h \in \tilde{V}_h^{nc}, b_h \in B_h, K \in \mathcal{T}_h, \mathbf{a} \in \mathbb{R}^2.$$

The validity of (6.2) and (6.3) is then obvious. \square

With respect to the $L^2(\Omega)$ norm, an analogous orthogonality result is generally not available. Nevertheless, transforming the functions v_h , b_h onto the reference element and using the equivalence of norms on finite-dimensional spaces, we can prove that

$$(6.4) \quad \|v_h\|_{0,\Omega} + \|b_h\|_{0,\Omega} \leq C \|v_h + b_h\|_{0,\Omega} \quad \forall v_h \in \tilde{V}_h^{nc}, b_h \in B_h.$$

Let the weak solution of (1.1) belong to $H^2(\Omega)$. Then it follows from (6.2) that

$$(6.5) \quad |u_h^{lin} - i_h u|_{1,h} \leq |u_h - i_h u|_{1,h},$$

and hence, with respect to $|\cdot|_{1,h}$, the function u_h^{lin} approximates the piecewise linear interpolate of u at least as well as u_h . Moreover, we obtain the following result.

THEOREM 6.2. *Let $u \in H^2(\Omega)$. Then*

$$(6.6) \quad |u - u_h^{lin}|_{1,h} \leq |u - u_h|_{1,h} + 2|u - i_h u|_{1,\Omega},$$

$$(6.7) \quad \|u - u_h^{lin}\|_{0,\Omega} \leq C \|u - u_h\|_{0,\Omega} + C \|u - i_h u\|_{0,\Omega},$$

$$(6.8) \quad \| \|u - u_h^{lin}\| \| \leq C \left(1 + \max_{K \in \mathcal{T}_h} \delta_K^{1/2}\right) (\| \|u - u_h\| \| + \| \|u - i_h u\| \|).$$

Proof. Inequality (6.6) is a direct consequence of (6.5). Analogously, using (6.4), we get (6.7). To prove (6.8), let us consider any $K \in \mathcal{T}_h$ and any $\mathbf{a} \in \mathbb{R}^2$. Applying (6.3), we deduce that

$$\begin{aligned} \|\mathbf{b} \cdot \nabla(i_h u - u_h^{lin})\|_{0,K} &\leq \|(\mathbf{b} - \mathbf{a}) \cdot \nabla(i_h u - u_h^{lin})\|_{0,K} + \|\mathbf{a} \cdot \nabla(i_h u - u_h)\|_{0,\Omega} \\ &\leq \|\mathbf{b} - \mathbf{a}\|_{0,\infty,K} (|i_h u - u_h^{lin}|_{1,K} + |i_h u - u_h|_{1,K}) + \|\mathbf{b} \cdot \nabla(i_h u - u_h)\|_{0,K}. \end{aligned}$$

Since $\inf_{\mathbf{a} \in \mathbb{R}^2} \|\mathbf{b} - \mathbf{a}\|_{0,\infty,K} \leq C h_K |\mathbf{b}|_{1,\infty,K}$, it follows from (3.4) that

$$\|\mathbf{b} \cdot \nabla(i_h u - u_h^{lin})\|_{0,K} \leq C (\|i_h u - u_h^{lin}\|_{0,K} + \|i_h u - u_h\|_{0,K}) + \|\mathbf{b} \cdot \nabla(i_h u - u_h)\|_{0,K}.$$

Now, using (6.6), (6.7), and the triangular inequality, we obtain (6.8). \square

The above estimates show that u_h^{lin} converges to the weak solution with the same convergence orders as u_h and that the estimate of Theorem 4.2 remains valid for u_h^{lin} . Therefore, it is possible and for practical reasons sensible to consider the piecewise linear part of u_h as a discrete solution of (1.1).

7. Numerical results. In this section, we present numerical results computed using either the discretization (3.2) or a discretization obtained from (3.2) by replacing a_h^{skew} by a_h^{conv} defined in (4.10). We used the P_1^{nc} element ($V_h = V_h^{nc}$) and the P_1^{mod} element ($V_h = V_h^{mod}$) defined using \widehat{b}_i given in (5.5). (We considered the basis functions presented in subsection 5.2.) For the P_1^{mod} element, we obtained almost identical results for a_h^{conv} and a_h^{skew} , and therefore we show only results obtained for the following three discretizations: a_h^{conv}/P_1^{nc} , a_h^{skew}/P_1^{nc} , and a_h^{skew}/P_1^{mod} .

The bilinear forms a_h^{skew} and a_h^{conv} were computed exactly, whereas the right-hand side l_h was evaluated using a quadrature formula which is exact for piecewise cubic f . The arising linear systems were solved applying the GMRES method with ILU preconditioning. The computations were terminated if the ratio of the norms of the residuum and the right-hand side was smaller than 10^{-8} .

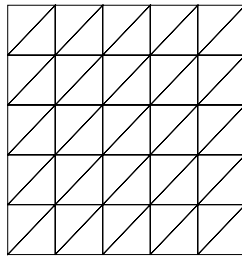


FIG. 7.1. Type of triangulations used in numerical computations.

All presented computational results were obtained for $\Omega = (0, 1)^2$ discretized using Friedrichs–Keller triangulations of the type depicted in Figure 7.1. We present results obtained for $h \doteq 7.07 \cdot 10^{-2}$, $h \doteq 3.54 \cdot 10^{-2}$, $h \doteq 1.77 \cdot 10^{-2}$, and $h \doteq 8.84 \cdot 10^{-3}$, which corresponds to 800, 3200, 12800, and 51200 elements, respectively. The errors of the discrete solutions were measured in the norms $\|\cdot\|_{0,\Omega}$, $|\cdot|_{1,h}$, $|||\cdot|||$ and in the discrete L^∞ norm $\|\cdot\|_{0,\infty,h}$ which is defined as the maximum of the errors in the midpoints of edges. The evaluation of $\|\cdot\|_{0,\Omega}$ (resp., $|\cdot|_{1,h}$) was exact for piecewise quadratic (resp., cubic) functions. For the P_1^{mod} element, we give the errors of the piecewise linear part u_h^{lin} of u_h . (See section 6.) The convergence orders were always computed using values from triangulations with $h \doteq 1.77 \cdot 10^{-2}$ and $h \doteq 8.84 \cdot 10^{-3}$.

The three discretizations were used to solve the convection–diffusion equation (1.1) for three types of solutions specified in Examples 7.1–7.3 below. The parameter δ_K was defined as in Remark 4.1 with $\kappa_K = 1$, $\kappa_K = 0.25$, and $\kappa_K = 0.2$, respectively. Examples 7.1 and 7.2 are the same as in [11] and [12].

EXAMPLE 7.1 (smooth polynomial solution). Let $\mathbf{b} = (3, 2)$, $c = 2$, and $u_b = 0$. For a given $\varepsilon > 0$, the right-hand side f is chosen such that

$$u(x, y) = 100 x^2 (1 - x)^2 y (1 - y) (1 - 2y)$$

is the exact solution of (1.1); see Figure 7.2.

For $\varepsilon = 1$, we observed optimal convergence orders for all three discretizations, and the errors of the discrete solutions were very similar. To investigate whether the methods are ε -uniform, i.e., whether an estimate of the type

$$|||u - u_h||| \leq C h^\nu \|u\|$$

holds with C and ν independent of ε , we considered $\varepsilon = h^\alpha$ for various values of α . Tables 7.1–7.3 show results obtained for $\alpha = 4$. We remark that the values of h

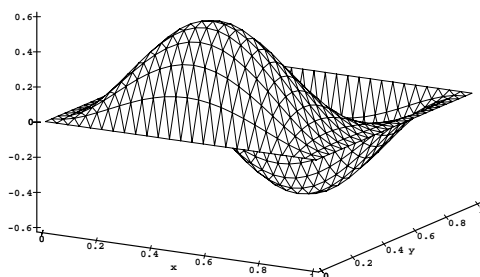


FIG. 7.2. Exact solution of Example 7.1.

and ε are rounded in all the tables. The solutions of the discretization a_h^{conv}/P_1^{nc} converge with the optimal order $3/2$ in the streamline diffusion norm $||| \cdot |||$, which is in correspondence with subsection 4.1. Note, however, that on unstructured meshes this optimal convergence order was not observed, which indicates that the constants α_h in (4.11) generally cannot be bounded from below by some $\alpha_0 > 0$ independent of h . The influence of the consistency error r_h^s with respect to ε can clearly be seen from Table 7.2: the solution of (3.2) with the P_1^{nc} element does not converge in $||| \cdot |||$, which is in agreement with Theorem 4.2. Table 7.3 shows that the P_1^{mod} element leads to best possible convergence orders which can be expected from a first order finite element space. Particularly, we observe the convergence order $3/2$ in the streamline

TABLE 7.1
Example 7.1; errors for a_h^{conv} with the P_1^{nc} element and $\varepsilon = h^4$.

h	ε	$\ \cdot \ _{0,\Omega}$	$ \cdot _{1,h}$	$ \cdot $	$\ \cdot \ _{0,\infty,h}$
7.07-2	2.50-5	1.49-2	1.40+0	1.43-1	6.87-2
3.54-2	1.56-6	5.86-3	1.09+0	5.10-2	3.88-2
1.77-2	9.77-8	2.07-3	7.57-1	1.80-2	2.20-2
8.84-3	6.10-9	6.94-4	4.98-1	6.36-3	1.20-2
conv. order		1.58	0.60	1.50	0.88

TABLE 7.2
Example 7.1; errors for a_h^{skew} with the P_1^{nc} element and $\varepsilon = h^4$.

h	ε	$\ \cdot \ _{0,\Omega}$	$ \cdot _{1,h}$	$ \cdot $	$\ \cdot \ _{0,\infty,h}$
7.07-2	2.50-5	4.56-1	4.29+1	7.79-1	1.89+0
3.54-2	1.56-6	4.32-1	8.66+1	7.43-1	1.71+0
1.77-2	9.77-8	4.27-1	1.78+2	7.09-1	1.47+0
8.84-3	6.10-9	4.37-1	3.72+2	6.86-1	1.53+0
conv. order		-0.03	-1.06	0.05	-0.06

TABLE 7.3
Example 7.1; errors for a_h^{skew} with the P_1^{mod} element and $\varepsilon = h^4$.

h	ε	$\ \cdot \ _{0,\Omega}$	$ \cdot _{1,h}$	$ \cdot $	$\ \cdot \ _{0,\infty,h}$
7.07-2	2.50-5	2.19-3	2.14-1	1.48-1	7.76-3
3.54-2	1.56-6	5.53-4	1.07-1	5.24-2	2.03-3
1.77-2	9.77-8	1.40-4	5.37-2	1.85-2	5.12-4
8.84-3	6.10-9	3.53-5	2.69-2	6.56-3	1.28-4
conv. order		1.99	1.00	1.50	2.00

TABLE 7.4

Example 7.1; comparison between a_h^{conv} with P_1^{nc} and a_h^{skew} with P_1^{mod} for $h \doteq 8.84 \cdot 10^{-3}$.

ε	$\ \cdot\ _{0,\Omega}$		$ \cdot _{1,h}$		$ \cdot $		$\ \cdot\ _{0,\infty,h}$	
	P_1^{nc}	P_1^{mod}	P_1^{nc}	P_1^{mod}	P_1^{nc}	P_1^{mod}	P_1^{nc}	P_1^{mod}
1-04	4.14-5	3.61-5	2.94-2	2.69-2	6.29-3	6.56-3	1.90-4	1.27-4
1-06	4.83-4	3.52-5	3.46-1	2.69-2	6.33-3	6.56-3	8.31-3	1.28-4
1-08	6.93-4	3.53-5	4.98-1	2.69-2	6.36-3	6.56-3	1.20-2	1.28-4
1-10	6.96-4	3.53-5	5.00-1	2.69-2	6.36-3	6.56-3	1.20-2	1.28-4

diffusion norm, which is again in agreement with our theory in section 4. The convergence orders are better than for a_h^{conv}/P_1^{nc} and a_h^{skew}/P_1^{nc} , and the discrete solutions obtained using the P_1^{mod} element are in all cases more accurate than P_1^{nc} solutions. Table 7.4 shows results obtained for various values of ε on a fixed triangulation. The errors for a_h^{skew}/P_1^{mod} are almost independent of ε in all norms, whereas the errors for a_h^{conv}/P_1^{nc} increase when ε decreases.

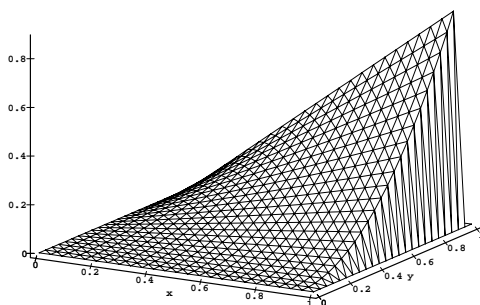


FIG. 7.3. Exact solution of Example 7.2.

EXAMPLE 7.2 (layers at the outflow part of the boundary). Let $\mathbf{b} = (2, 3)$ and $c = 1$. For a given $\varepsilon > 0$, the right-hand side f and the boundary condition u_b are chosen such that

$$u(x, y) = x y^2 - y^2 \exp\left(\frac{2(x-1)}{\varepsilon}\right) - x \exp\left(\frac{3(y-1)}{\varepsilon}\right) + \exp\left(\frac{2(x-1) + 3(y-1)}{\varepsilon}\right)$$

is the exact solution of (1.1). This function has boundary layers at $x = 1$ and $y = 1$; see Figure 7.3.

All three discretizations gave identical errors in $|||\cdot|||$ with convergence order 1.00 and in $|\cdot|_{1,h}$ with convergence order 0.50. The reduction of the convergence order

TABLE 7.5

Example 7.2; comparison between all three discretizations for $\varepsilon = 10^{-8}$.

h	$\ \cdot\ _{0,\Omega}$			$\ \cdot\ _{0,\infty,h}$		
	a_h^{conv} P_1^{nc}	a_h^{skew} P_1^{nc}	a_h^{skew} P_1^{mod}	a_h^{conv} P_1^{nc}	a_h^{skew} P_1^{nc}	a_h^{skew} P_1^{mod}
7.07-2	1.32+0	7.54-1	8.72-2	9.21+0	3.65+0	6.08-1
3.54-2	1.92+0	8.23-1	6.22-2	1.89+1	4.74+0	6.37-1
1.77-2	2.74+0	8.70-1	4.42-2	3.84+1	5.72+0	6.52-1
8.84-3	3.89+0	8.98-1	3.13-2	7.72+1	6.50+0	6.60-1
order	-0.50	-0.05	0.50	-1.01	-0.18	-0.02

TABLE 7.6

Example 7.2; errors for a_h^{conv} with the P_1^{nc} element and $\varepsilon = 10^{-8}$.

h	$\ \cdot\ _{0,\Omega}^*$	$ \cdot _{1,h}^*$	$ \cdot $	$\ \cdot\ _{0,\infty,h}^*$
7.07-2	2.53-2	2.83+0	2.99-2	1.93-1
3.54-2	9.20-4	2.03-1	2.87-3	9.07-3
1.77-2	9.75-5	4.02-2	9.62-4	2.93-4
8.84-3	2.42-5	1.99-2	3.39-4	7.14-5
order	2.01	1.01	1.50	2.04

TABLE 7.7

Example 7.2; errors for a_h^{skew} with the P_1^{nc} element and $\varepsilon = 10^{-8}$.

h	$\ \cdot\ _{0,\Omega}^*$	$ \cdot _{1,h}^*$	$ \cdot $	$\ \cdot\ _{0,\infty,h}^*$
7.07-2	3.09-1	3.47+1	3.36-1	1.31+0
3.54-2	3.13-1	6.98+1	3.22-1	1.33+0
1.77-2	3.14-1	1.40+2	3.19-1	1.31+0
8.84-3	3.15-1	2.80+2	3.18-1	1.31+0
order	0.00	-1.00	0.00	0.00

TABLE 7.8

Example 7.2; errors for a_h^{skew} with the P_1^{mod} element and $\varepsilon = 10^{-8}$.

h	$\ \cdot\ _{0,\Omega}^*$	$ \cdot _{1,h}^*$	$ \cdot $	$\ \cdot\ _{0,\infty,h}^*$
7.07-2	1.69-3	3.54-2	1.48-2	1.74-2
3.54-2	4.05-5	8.80-3	2.78-3	4.37-4
1.77-2	8.63-6	4.37-3	9.79-4	2.93-5
8.84-3	2.16-6	2.19-3	3.46-4	7.37-6
order	2.00	1.00	1.50	1.99

is caused by the interpolation error in the boundary layer region since the thickness of the layers is smaller than h for all triangulations used. The errors in $\|\cdot\|_{0,\Omega}$ and $\|\cdot\|_{0,\infty,h}$ are shown in Table 7.5. The errors for a_h^{conv}/P_1^{nc} increase for decreasing h and the errors for a_h^{skew}/P_1^{nc} do not change significantly. For a_h^{skew}/P_1^{mod} , the discrete solution converges in $\|\cdot\|_{0,\Omega}$ with order 0.50. Since the boundary layer is not resolved by the mesh, no convergence is observed in the maximum norm.

The streamline diffusion method with conforming finite element approximations is known to approximate solutions with layers on nonlayer-adapted meshes at least outside the layers very precisely. Tables 7.6–7.8 show the behavior of the discrete solutions outside the boundary layers in the domain $\Omega^* = (0, 0.8)^2$. The discretizations a_h^{conv}/P_1^{nc} and a_h^{skew}/P_1^{mod} give optimal convergence orders, but a_h^{skew}/P_1^{mod} is about 10 times more accurate than a_h^{conv}/P_1^{nc} in all norms except for $|||\cdot|||$. Table 7.7 shows that the discretization a_h^{skew}/P_1^{nc} is completely useless.

EXAMPLE 7.3 (inner and boundary layers). We set $\mathbf{b} = (1/2, \sqrt{3}/2)$, $c = 0$, $f = 0$, and

$$u_b(x, y) = \begin{cases} 0 & \text{for } x \geq 1/2 \text{ or } y = 1, \\ 1 & \text{else.} \end{cases}$$

For $\varepsilon \rightarrow 0$, the solution u of (1.1) tends to the function

$$u^0(x, y) = \begin{cases} 0 & \text{for } y \leq \sqrt{3}(x - 1/2), \\ 1 & \text{else,} \end{cases}$$

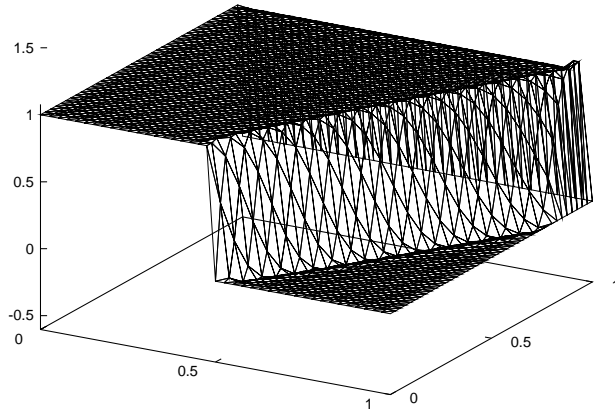


FIG. 7.4. Solution of Example 7.3 for $h \doteq 3.54 \cdot 10^{-2}$.

which is the solution of the hyperbolic limit of (1.1). Thus, for small ε , the solution u has an inner layer along the line $y = \sqrt{3}(x - 1/2)$ and boundary layers along $y = 1$ and $x = 1, y > \sqrt{3}/2$. We consider $\varepsilon = 10^{-6}$ below.

This example does not fit into the theory presented in this paper, particularly since $u_b \notin H^{3/2}(\partial\Omega)$. However, it is a challenging test case which can indicate the quality of numerical methods for solving (1.1).

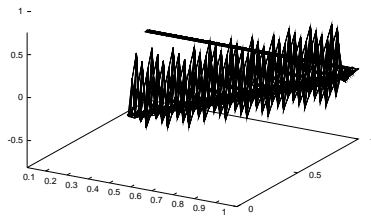


FIG. 7.5. Example 7.3; errors larger than 0.01 for $h \doteq 1.77 \cdot 10^{-2}$.

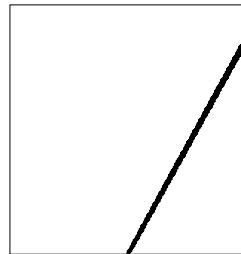


FIG. 7.6. Example 7.3; region of errors larger than 0.1 for $h \doteq 8.84 \cdot 10^{-3}$.

Figures 7.4–7.6 show results computed using the discrete problem (3.2) with the P_1^{mod} element. Instead of showing the discontinuous solution u_h directly, we present a corresponding conforming function $\tilde{u}_h \in \tilde{V}_h^{conf}$ such that the value of \tilde{u}_h at any inner vertex is equal to the arithmetic mean value of the values of u_h at the midpoints of edges connected with this vertex. The errors of \tilde{u}_h in Figures 7.5 and 7.6 were computed using the limit solution u^0 . We see that inner and boundary layers are detected very well and that the method behaves in a robust way, although the assumptions made in section 1 are not satisfied.

We can conclude that in all numerical tests we have performed, the P_1^{mod} element always led to optimal convergence orders and behaved very robustly with respect to ε . The accuracy of solutions obtained using the P_1^{mod} element was always better than

for the P_1^{nc} element and, moreover, the iterative solver used to compute the discrete solutions converged much faster for the P_1^{mod} element than for discretizations using the P_1^{nc} element. Thus, the P_1^{mod} element not only improves the stability of the discrete solution but also the convergence properties of the solver.

REFERENCES

- [1] F. BREZZI, D. MARINI, AND E. SÜLI, *Residual-free bubbles for advection-diffusion problems: The general error analysis*, Numer. Math., 85 (2000), pp. 31–47.
- [2] F. BREZZI, T. J. R. HUGHES, L. D. MARINI, A. RUSSO, AND E. SÜLI, *A priori error analysis of residual-free bubbles for advection-diffusion problems*, SIAM J. Numer. Anal., 36 (1999), pp. 1933–1948.
- [3] P. G. CIARLET, *Basic Error Estimates for Elliptic Problems*, in Handbook of Numerical Analysis, Vol. 2—Finite Element Methods (pt. 1), P. G. Ciarlet and J. L. Lions, eds., North-Holland, Amsterdam, 1991, pp. 17–351.
- [4] M. CROUZEIX AND P.-A. RAVIART, *Conforming and nonconforming finite element methods for solving the stationary Stokes equations I*, Rev. Franc. Automat. Inform. Rech. Operat., 7 (1973), R-3, pp. 33–76.
- [5] O. DOROK, V. JOHN, U. RISCH, F. SCHIEWECK, AND L. TOBISKA, *Parallel finite element methods for the incompressible Navier–Stokes equations*, in Flow Simulation with High-Performance Computers II, Notes Numer. Fluid Mech. 52, E. H. Hirschel, ed., Vieweg-Verlag, Braunschweig, Wiesbaden, 1996, pp. 20–33.
- [6] K. ERIKSSON AND C. JOHNSON, *Adaptive streamline diffusion finite element methods for stationary convection-diffusion problems*, Math. Comp., 60 (1993), pp. 167–188.
- [7] M. FORTIN AND M. SOULIE, *A non-conforming piecewise quadratic finite element on triangles*, Internat. J. Numer. Methods Engrg., 19 (1983), pp. 505–520.
- [8] T. J. R. HUGHES AND A. N. BROOKS, *A multi-dimensional upwind scheme with no crosswind diffusion*, in Finite Element Methods for Convection Dominated Flows, AMD 34, T. J. R. Hughes, ed., ASME, New York, 1979, pp. 19–35.
- [9] V. JOHN, *Parallele Lösung der inkompressiblen Navier–Stokes Gleichungen auf adaptiv verfeinerten Gittern*, Ph.D. thesis, Otto-von-Guericke-Universität Magdeburg, Magdeburg, Germany, 1997.
- [10] C. JOHNSON AND J. SARANEN, *Streamline diffusion methods for the incompressible Euler and Navier–Stokes equations*, Math. Comp., 47 (1986), pp. 1–18.
- [11] V. JOHN, G. MATTHIES, F. SCHIEWECK, AND L. TOBISKA, *A streamline-diffusion method for nonconforming finite element approximations applied to convection-diffusion problems*, Comput. Methods Appl. Mech. Engrg., 166 (1998), pp. 85–97.
- [12] V. JOHN, J. M. MAUBACH, AND L. TOBISKA, *Nonconforming streamline-diffusion-finite-element-methods for convection-diffusion problems*, Numer. Math., 78 (1997), pp. 165–188.
- [13] P. KNOBLOCH, *On Korn’s inequality for nonconforming finite elements*, Technische Mechanik, 20 (2000), pp. 205–214 and 375 (errata).
- [14] K. NIJIMA, *Pointwise error estimates for a streamline diffusion finite element scheme*, Numer. Math., 56 (1990), pp. 707–719.
- [15] H.-G. ROOS, M. STYNES, AND L. TOBISKA, *Numerical Methods for Singularly Perturbed Differential Equations. Convection-Diffusion and Flow Problems*, Springer-Verlag, Berlin, 1996.
- [16] F. SCHIEWECK, *Parallele Lösung der stationären inkompressiblen Navier–Stokes Gleichungen*, Habilitationsschrift, Otto-von-Guericke-Universität Magdeburg, Magdeburg, Germany, 1997.
- [17] M. STYNES AND L. TOBISKA, *The streamline-diffusion method for nonconforming Q_1^{rot} elements on rectangular tensor-product meshes*, IMA J. Numer. Anal., 21 (2001), pp. 123–142.
- [18] L. TOBISKA AND R. VERFÜRTH, *Analysis of a streamline diffusion finite element method for the Stokes and Navier–Stokes equations*, SIAM J. Numer. Anal., 33 (1996), pp. 107–127.